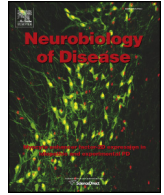




Contents lists available at ScienceDirect

Neurobiology of Disease

journal homepage: www.elsevier.com/locate/ynbdi

Q1 Oxidative stress and lipid peroxidation are upstream of 2 amyloid pathology

Q2 Muriel Arimon¹, Shuko Takeda, Kathryn L. Post², Sarah Svirsky, Bradley T. Hyman, Oksana Berezovska*

4 MassGeneral Institute for Neurodegenerative Disease, Department of Neurology, Massachusetts General Hospital, Harvard Medical School, CNY 114, 16th Street, Charlestown 02129, MA, USA

5 A R T I C L E I N F O

6 Article history:
7 Received 20 January 2015
8 Revised 11 June 2015
9 Accepted 17 June 2015
10 Available online xxx

11 Keywords:
12 Oxidative stress
13 Lipid peroxidation
14 Alzheimer's disease
15 Microdialysis
16 Amyloid beta
17 γ -Secretase
18 Presenilin
19 4-Hydroxynonenal

A B S T R A C T

Oxidative stress is a common feature of the aging process and of many neurodegenerative disorders, including Alzheimer's disease. Understanding the direct causative relationship between oxidative stress and amyloid pathology, and determining the underlying molecular mechanisms is crucial for the development of more effective therapeutics for the disease. By employing microdialysis technique, we report local increase in the amyloid- β_{42} levels and elevated amyloid- $\beta_{42/40}$ ratio in the interstitial fluid within 6 h of direct infusion of oxidizing agents into the hippocampus of living and awake wild type mice. The increase in the amyloid- $\beta_{42/40}$ ratio correlated with the pathogenic conformational change of the amyloid precursor protein-cleaving enzyme, presenilin1/ γ -secretase. Furthermore, we found that the product of lipid peroxidation 4-hydroxynonenal, binds to both nicastrin and BACE, differentially affecting γ - and β -secretase activity, respectively. The present study demonstrates a direct cause-and-effect correlation between oxidative stress and altered amyloid- β production, and provides a molecular mechanism by which naturally occurring product of lipid peroxidation may trigger generation of toxic amyloid- β_{42} species.

© 2014 Published by Elsevier Inc.

34
35

37 1. Introduction

38 Alzheimer's disease (AD) is an age-related neurodegenerative disorder characterized clinically by progressive memory loss and cognitive decline. The major neuropathological hallmarks of AD are neuronal and synapse loss, accumulation of intraneuronal fibrillary tangles, and deposition of extracellular amyloid plaques consisting of amyloid- β peptide (A β) (Hardy and Selkoe, 2002). A β generation is mediated by sequential cleavage of the amyloid precursor protein (APP) by β -secretase (BACE) and γ -secretase. The latter is an enzymatic complex composed of presenilin (PS1 or PS2), nicastrin (NCT), Aph-1 and presenilin enhancer-2 (Pen2) (Bergmans and De Strooper, 2010). Familial early-onset AD (FAD) is caused by autosomal dominant mutations in presenilin (*PSEN1* and *PSEN2*) and APP genes. However, the sporadic late onset form of AD (SAD) represents the vast majority of the

cases, and yet its etiology remains poorly understood. The major non-genetic risk factor involved in the pathogenesis of SAD is aging, which is often accompanied by accumulation of reactive oxygen species (ROS) (Finkel and Holbrook, 2000). ROS are generated as a result of normal intracellular metabolism and may function as signaling molecules (Nemoto et al., 2000; Nishikawa et al., 2000). At the same time, a number of external agents such as ultraviolet light or environmental toxins, or internal inflammatory processes can trigger excessive ROS production (Finkel and Holbrook, 2000). An imbalance due to either increased ROS production or decreased antioxidant defense mechanisms leads to oxidative stress, which damages various cell components via modification of proteins, lipids and DNA, and disrupts numerous cellular processes.

Oxidative damage can be observed in the brain of patients with mild cognitive impairment (MCI) (Lovell and Markesbery, 2001; Butterfield et al., 2006), a transition stage between normal aging and dementia, and is detected at the early stages of AD (Mangialasche et al., 2009; Reed et al., 2009a, 2009b; Sultana and Butterfield, 2010; Sun, 2010; Subramanian et al., 2011). It has been reported that the level of antioxidant enzymes is diminished, whereas inflammation, ROS production, and the level of oxidative stress markers are elevated in the brain of AD patients, compared to that in the age-matched controls (Sultana and Butterfield, 2010; Krstic and Knuesel, 2013). Specifically, 4-hydroxynonenal (HNE), an aldehyde product of lipid peroxidation, has been shown to accumulate in the brain due to normal aging, and is present at high levels and believed to be associated with amyloid

Abbreviations: A β , amyloid beta; DTDP, 4,4'-dithiodipyridine; HNE, 4-hydroxynonenal; EFRET, Fluorescence Resonance Energy Transfer efficiency; FLIM, Fluorescence Lifetime Imaging Microscopy; NACA, N-acetylcysteine amide; PS1, presenilin 1.

* Corresponding author at: MassGeneral Institute for Neurodegenerative Disease (MIND), Massachusetts General Hospital, Harvard Medical School, 114 16th Street, Charlestown, MA 02129, USA. Fax: +1 617 724 1480.

E-mail address: OBerezovska@partners.org (O. Berezovska).

¹ Current address: Institut de Neurociències, Departament de Bioquímica i Biologia Molecular, Universitat Autònoma de Barcelona, 08193 Bellaterra, Spain.

² Current address: Brain Research Center, University of British Columbia, Vancouver, BC V6T2B5, Canada.

Available online on ScienceDirect (www.sciencedirect.com).

<http://dx.doi.org/10.1016/j.nbd.2015.06.013>
0969-9961/© 2014 Published by Elsevier Inc.

Please cite this article as: Arimon, M., et al., Oxidative stress and lipid peroxidation are upstream of amyloid pathology, Neurobiol. Dis. (2014), <http://dx.doi.org/10.1016/j.nbd.2015.06.013>

pathology in MCI and AD patients (Sajdel-Sulkowska and Marotta, 1984; Butterfield et al., 1997, 2006; Shichiri et al., 2011; Subramanian et al., 2011; Chavez-Gutierrez et al., 2012). Interestingly, lipid peroxidation can be detected prior to A β deposition in a mouse model of AD (Pratico et al., 2001), suggesting that it may be upstream of A β pathology. On the other hand, increased oxidative stress has been found in the vicinity of amyloid plaques (McLellan et al., 2003; Garcia-Alloza et al., 2006; Xie et al., 2013) and A β peptide itself has been shown to trigger increase in oxidative stress (Harris et al., 1995; Butterfield, 2002; Butterfield et al., 2002; Atamna and Boyle, 2006; Cai et al., 2011). However, the causality and interrelationship between oxidative stress and A β pathology remains poorly understood.

To determine whether oxidative stress may be an initiator of A β pathology, we employed *in vivo* microdialysis to locally induce acute oxidative stress in the brain of living mice. We provide evidence of a direct causative role of oxidative stress, and specifically lipid peroxidation, in promoting A β 42 production and increasing the A β 42/40 ratio in the brain of wild type mice. We report that HNE covalently modifies nicastrin (NCT) in the γ -secretase complex as well as BACE, via the formation of HNE adducts. These covalent modifications result in altered γ - and β -secretase activities, and cause pathogenic conformational change in PS1/ γ -secretase associated with altered APP processing.

2. Materials and methods

2.1. *In vivo* microdialysis

In vivo microdialysis sampling of brain interstitial A β was performed as described previously (Wolfe, 2007; Takeda et al., 2011). The microdialysis probes used had a 4 mm shaft with a 3.0 mm, 1000 kDa molecular weight cutoff (MWCO) polyethylene (PE) membrane (PEP-4-03, Eicom, Kyoto, Japan). Before use, the probe was conditioned by briefly dipping it in ethanol, and then washed with sterile artificial cerebrospinal fluid (ACSF) perfusion buffer (122 mM NaCl, 1.3 mM CaCl₂, 1.2 mM MgCl₂, 3.0 mM KH₂PO₄, 25.0 mM NaHCO₃). The preconditioned probe's outlet and inlet were connected to a peristaltic pump (ERP-10, Eicom, Kyoto, Japan) and a microsyringe pump (ESP-32, Eicom, Kyoto, Japan), respectively, using fluorinated ethylene propylene (FEP) tubing (\varnothing 250 μ m i.d.). Probe implantation was performed as previously described (Cirrito et al., 2003; Takeda et al., 2011), with slight modifications. Briefly, the animals were anesthetized with isoflurane, while a guide cannula (PEG-4, Eicom, Kyoto, Japan) was stereotactically implanted in both hippocampi (bregma -3.1 mm, 2.8 mm lateral to midline, -1.2 mm ventral to dura). The guide was fixed using binary dental cement. Three days after guide cannula implantation, the mice were placed in a standard microdialysis cage and a probe was inserted through the guide. After insertion of the probe, in order to obtain stable baseline recordings, the probe and connecting tubes were perfused with ACSF for 180 min at a flow rate of 10 μ l/min before baseline sample collection. First, a baseline sample was collected for 180 min before the delivery of either 3 mM 4,4'-dithiodipyridine (DTDP) (Sigma-Aldrich) or 5 mM 4-hydroxynonenal (HNE) (Cayman Chemical, Ann Arbor, MI) in the right hemisphere, or vehicle EtOH as a control in the left hemisphere. Samples were collected from the brain of mice at 180 min intervals at a flow rate of 0.5 μ l/min. The antioxidant N-acetylcysteine amide (NACA) (Sigma-Aldrich) diluted in DMSO was delivered at 7.5 mM for 12 hours prior to the oxidative stress. During microdialysis sample collection, mice were awake and freely moving in the microdialysis cage designed to allow unrestricted movement of the animals without applying pressure on the probe assembly (AtmosLM microdialysis system, Eicom, Kyoto, Japan).

2.2. A β quantification

A β 40 and A β 42 concentrations were determined by Human/Rat β Amyloid (40 or 42) sandwich ELISA (Wako Pure Chemicals Industries,

Osaka, Japan), according to the manufacturer's instructions. To dissociate oligomerized A β , samples were incubated with 500 mM guanidine HCl for 30 min at room temperature.

2.3. Immunohistochemistry

Following the microdialysis, mouse brains were removed and post-fixed in 4% paraformaldehyde (PFA) solution for 72 hours, cryoprotected in 30% sucrose, 30% (v/v) ethylene glycol in 0.1 M PBS and sectioned on a freezing microtome at 35 μ m thickness. The free-floating brain tissue sections were washed with PBS and permeabilized in blocking buffer (1.5% Normal Donkey Serum, 0.4% Triton-X100 in PBS) for 60 minutes. Samples were then incubated overnight at 4 $^{\circ}$ C with the respective primary antibodies (goat PS1-N-Terminus (NT), Millipore; rabbit PS1-C-Terminus (CT), Sigma-Aldrich) in blocking buffer (1.5% Normal Donkey Serum, 0.1% Triton-X100 in PBS). Alexa488- and Cy3-conjugated secondary antibodies (donkey-anti-goat AlexaFluor488, Invitrogen; donkey-anti-rabbit Cy3, Jackson ImmunoResearch) were used for detection. Sections were coverslipped with Vectashield mounting medium without DAPI (Vector Laboratories), sealed, and stored at 4 $^{\circ}$ C until imaged.

2.4. Fluorescence lifetime imaging microscopy (FLIM)

The relative proximity between fluorescently labeled PS1 N- and C-termini, as a measure of PS1 conformation, was monitored using Fluorescence Lifetime Imaging microscopy (FLIM), as previously described (Lleo et al., 2004; Berezovska et al., 2005). Briefly, mouse brain sections immunostained with Alexa488 (A488) as the donor fluorophore to label PS1 NT and Cy3 as the acceptor fluorophore to label PS1 CT (see above) were imaged on the LSM510 Zeiss microscope equipped with Becker & Hickl (Berlin, Germany) hardware and software. Donor fluorophore lifetimes were measured using multi-exponential analysis to distinguish between PS1 molecules in different conformational states as described in detail previously (Wahlster et al., 2013). The Fluorescence Resonance Energy Transfer efficiency (%E_{FRET}) reflecting PS1 NT-CT proximity was calculated as the percent of decrease in the baseline lifetime of the A488 donor fluorophore due to presence of the Cy3-acceptor fluorophore in close proximity using the following equation:

$$\%E_{\text{FRET}} = 100 * (t_1 - t_2) / t_1$$

where t₁ is the lifetime of the A488 donor fluorophore alone (FRET absent), and t₂ is the A488 lifetime in the presence of Cy3 (FRET present). The FRET efficiency values could be color-coded to show distribution of neurons with PS1 in different conformational states within the CA1 area of hippocampus after the treatment. Yellow-to-red pixels represent high %E_{FRET} ("closed" PS1 conformation), whereas green-blue pixels represent low %E_{FRET} ("open" PS1 conformation).

2.5. Membrane-enriched fractions from mouse brains and cell free γ -secretase assay

Wild-type mouse brain tissue was homogenized in buffer A (50 mM MES pH 6.0, 150 mM KCl, 5 mM MgCl₂, 5 mM CaCl₂) containing complete protease inhibitor mixture (Roche) with a teflon homogenizer, and cell debris and nuclei were removed by centrifugation at 800 \times g for 10 min. Supernatants were then centrifuged at 100,000 \times g for 60 min, resulting pellets were resuspended in ice cold carbonate buffer (100 mM Na₂CO₃ pH 11.2), and the centrifugation was repeated. Pellets were resuspended in buffer B (50 mM Hepes pH 7.0, 150 mM KCl, 5 mM MgCl₂, 5 mM CaCl₂), and the centrifugation was repeated. Membrane enriched fractions were solubilized in buffer B + 1% CHAPSO for 60 min at 4 $^{\circ}$ C, and centrifuged at 100,000 \times g for 60 min. All procedures were performed at 4 $^{\circ}$ C and the membranes suspensions were stored at -80 $^{\circ}$ C. Resulting supernatants are referred to as membrane-enriched

195 fractions. Membrane-enriched fractions (0.125 mg/ml) were incubated
 196 with human C100-Flag (1 μ M) in buffer B containing 0.25% CHAPSO at
 197 37 °C for 4 h. Negative controls were incubated either at 4 °C or at
 198 37 °C with the γ -secretase inhibitor (GSI) L-685,458 (50 nM,
 199 Calbiochem). Reaction was stopped by placing the samples in ice.

200 2.6. Cell lines and primary neuronal cultures

201 HEK293 cells were transfected with C99-flag construct (Uemura
 202 et al., 2010) using Lipofectamine 2000 reagent (Life Technologies) and
 203 were treated 24 h post-transfection. GFP plasmid was co-transfected
 204 along as a control for transfection efficiency.

205 Primary neuronal cultures were obtained from cerebral cortex of
 206 mouse embryos at gestation day 14–16 (Charles River Laboratories,
 207 Wilmington, MA), as described previously (Berezovska et al., 1999).
 208 Briefly, the dissected tissue was dissociated by trypsinization for 5 mi-
 209 nutes and re-suspended in neurobasal medium (Gibco, Invitrogen, Gai-
 210 thersburg, MD) supplemented with 10% fetal bovine serum (Gibco,
 211 Invitrogen), 2 mM/L L-glutamine (Gibco, Invitrogen), 100 U/mL penicil-
 212 lin and 100 μ g/mL streptomycin (Gibco, Invitrogen). Neurons were plat-
 213 ed in 35-mm glass bottom culture dishes (MatTek Corporation, Ashland,
 214 MA) previously coated with Poly-D-lysine hydrobromide at 100 μ g/ml
 215 (Sigma-Aldrich, St. Louis, MO) and cultures were maintained at 37 °C
 216 with 5% CO₂. Media was changed after 2 h to neurobasal medium sup-
 217 plemented with 2% B27 (Gibco, Invitrogen), 2 mM L-glutamine, penicil-
 218 lin and streptomycin. Neurons were cultured for 7–14 days *in vitro*
 219 before the treatment.

220 2.7. In vitro drug treatment

221 To induce oxidative stress, primary neurons were treated with either
 222 100 μ M DTDP or 1 mM HNE (both diluted in ethanol) for 20 min or 3 h.
 223 γ -secretase inhibitor DAPT (Sigma) was used overnight at 1 μ M
 224 concentration.

225 2.8. Immunoprecipitation and immunoblotting

226 For immunoprecipitation, primary neurons were washed with ice-
 227 cold PBS and were collected in lysis buffer (50 mM HEPES pH 7.4,
 228 100 mM NaCl, 0.1 mM EDTA, 1% (w/v) CHAPSO) containing complete
 229 protease inhibitor mixture (Roche). Samples were passed through a
 230 27G needle and incubated 1 h at 4 °C to completely solubilize
 231 membranes. After centrifugation at 20,000 \times g for 20 min, protein con-
 232 centration was determined in the resultant supernatant (solubilized
 233 membranes). Samples were pre-cleared with 20 μ l of protein-G
 234 Sepharose beads (Invitrogen) for 2 h at 4 °C. After removing the beads
 235 by centrifugation, supernatants were incubated with anti-PS1-NT
 236 (Millipore #AB1575) and anti-PS1-loop (Millipore #MAB5232) anti-
 237 bodies, or control IgGs (normal goat and mouse serum, Jackson
 238 ImmunoResearch) for 12/24 h at 4 °C. Next day, protein-G Sepharose
 239 beads were added to the samples for 1–2 h. After several washes
 240 with lysis buffer, immunoprecipitated samples were eluted by incuba-
 241 tion with sample buffer for 10 min at 95 °C, and applied to SDS-
 242 polyacrylamide gels.

243 For Western blotting, cells were washed with ice-cold PBS and then
 244 were incubated with lysis buffer (50 mM HEPES pH 7.4, 100 mM NaCl,
 245 0.1 mM EDTA, 1% Triton-X 100) containing complete protease inhibitor
 246 mixture (Roche). Cells were sonicated and centrifuged at 20,000 \times g for
 247 20 min at 4 °C before determining protein concentration. Samples
 248 were incubated with sample buffer for 5 min at 95 °C, applied to SDS-
 249 polyacrylamide gels (SDS-PAGE) and transferred to nitrocellulose
 250 membranes (0.1 μ m – 0.2 μ m pore size, Whatman). Membranes were
 251 probed with the following antibodies: anti-FLAG (1:2000, Wako), GFP
 252 (1:2000, Abcam), actin (1:2000, Abcam), nicastrin (1:1000, Sigma),
 253 HNE (1:500, Abcam), BACE (1:1000, Cell Signaling), 6E10 (1:1000,
 254 Covance), anti-mouse/rat APP (597) (corresponding to A β 1–16)

(1:100, IBL). Either horseradish peroxidase (HRP)-conjugated (1:2000,
 255 Bio-Rad) or infrared (IR)-dye conjugated (1:7500, IRDye680 or 800,
 256 Li-Cor Biosciences) secondary antibodies were used. Quantification of
 257 band density was determined by densitometric analysis in ImageJ soft-
 258 ware (National Institutes of Health). 259

260 2.9. Statistical analysis

261 Statistical analyses were performed using Graph Pad Prism software
 262 (GraphPad Software Inc., La Jolla, CA). Data is expressed as mean \pm SEM.
 263 D'Agostino & Pearson omnibus normality test was used to evaluate the
 264 normality of the distributions of values. Two-sided Student's *t* test was
 265 used for 2-group comparisons. The microdialysis data were analyzed
 266 using two-way ANOVA with repeated measures and Bonferroni post-
 267 test. Values were considered significant at **p* < 0.05. Higher significance
 268 is indicated as follows: ***p* < 0.01, ****p* < 0.001. 269

270 3. Results

271 3.1. Locally induced oxidative stress in vivo triggers local increase in A β 42 levels and A β 42/40 ratio

272 To determine the effect of oxidative stress on A β , we locally deliv-
 273 ered oxidizing agents into the brain of living and awake mice using mi-
 274 crodialysis technique. The levels of A β 40 and A β 42 were concomitantly
 275 quantified in the collected interstitial fluid (ISF). Two microdialysis
 276 probes were surgically implanted into the brain of ~12 months old
 277 wild-type mice, one probe into each hemisphere targeted to hippocam-
 278 pus (Fig. 1A). One probe was used to deliver the oxidizing agent (right
 279 hemisphere), and the contralateral side (left hemisphere) received infu-
 280 sion of the vehicle control. Two different compounds were used: 4,4'-
 281 dithiodipyridine (DTDP), a strong cell-permeant thiol-reactive agent in-
 282 ducing oxidative stress, and 4-hydroxynonenal (HNE), a naturally oc-
 283 ccurring aldehyde by-product of lipid peroxidation (see Supplementary
 284 Fig. 4 for detailed chemical structure). We used 3 mM DTDP and
 285 5 mM HNE for *in vivo* infusion since it is estimated that only around
 286 10–15% of the drug is delivered across the microdialysis probe mem-
 287 brane into ISF at the 0.5 μ l/min flow rate (Takeda et al., 2011), and is
 288 diluted further as it diffuses through the interstitial fluid. After establish-
 289 ing a baseline of A β levels for each individual animal/hemisphere
 290 (see Materials and Methods), DTDP or HNE diluted in artificial cerebro-
 291 spinal fluid (ACSF) were delivered into the brain, and ISF samples were
 292 collected after 3 h and 6 h of infusion for A β ELISA quantification
 293 (Fig. 1A).

294 A significant increase in the levels of both A β 40 and A β 42 was ob-
 295 served after 3 h and 6 h of DTDP treatment, with an increase in the
 296 A β 42/40 ratio as compared to the vehicle-treated contralateral hemi-
 297 sphere (Fig. 1B). Treatment with HNE triggered an increase in the
 298 A β 42 levels only, with no significant changes in the A β 40, leading to
 299 an even higher increase in the A β 42/40 ratio (Fig. 1C).

300 Increased susceptibility to oxidative stress are known to occur dur-
 301 ing aging (Finkel and Holbrook, 2000). Therefore, we next compared
 302 the extent of the effect of strong oxidant DTDP on A β 42 levels in
 303 4-month old (young) and compared them to that in 12 month-old
 304 (old) mice. We found that after 3 h of treatment, young animals
 305 displayed the same increase in the A β 40 and A β 42 levels as the old an-
 306 imals (Fig. 2 vs Fig. 1B). However, a significant recovery of both A β 40
 307 and A β 42 levels was observed in young animals after 6 h of DTDP treat-
 308 ment, with the level of A β 42 returning to that of the vehicle-treated
 309 hemisphere, which was not the case for old animals. Of note, young an-
 310 imals did not exhibit any change in the A β 42/40 ratio after either 3 h or
 311 6 h of DTDP treatment (Fig. 2). These data indicate that young animals
 312 are more resilient to the acute oxidative stress insults, which old an-
 313 imals are not able to overcome.

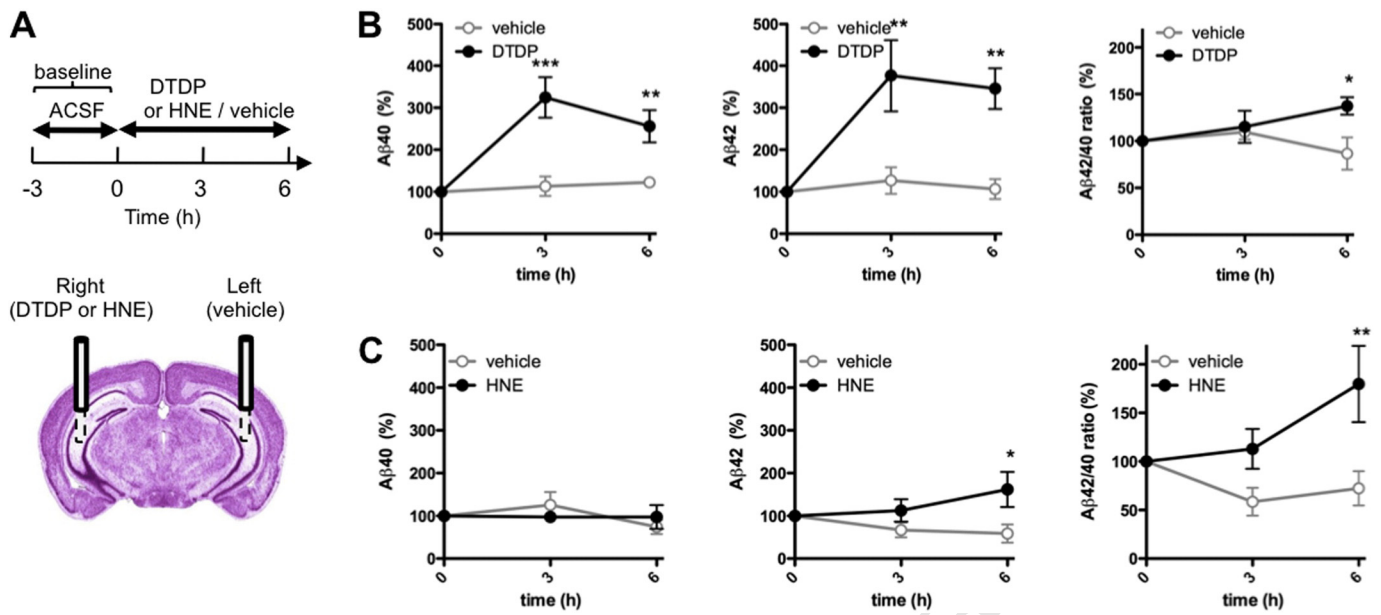


Fig. 1. Locally induced oxidative stress *in vivo* alters Aβ levels in wild-type mice. (A) Scheme of the time frame for DTDP, HNE or vehicle treatments delivered via microdialysis probe into hippocampus of 12 months old mice. (B–C) Levels of Aβ40 and Aβ42 in the ISF and the Aβ42/40 ratio after DTDP (B) or HNE (C) treatment were compared to that in the vehicle treated hemisphere of the same mouse (n = 5 animals). The baseline levels of ISF Aβ40 and Aβ42 collected prior to the treatment were 15.61 ± 1.35 pM and 6.31 ± 0.62 pM, respectively. Data represent the mean ± SEM, presented as percentage values relative to the time point zero of each hemisphere. Two-way ANOVA, Bonferroni posttest. *p < 0.05, **p < 0.01, ***p < 0.001, compared to the same time point of the vehicle-treated hemisphere.

314 3.2. Oxidative stress and lipid peroxidation induce a change in
315 PS1 conformation

316 We have previously established that changes in the Aβ42/40 ratio
317 closely correlate with changes in the conformation of PS1 in cells
318 *in vitro* (Berezovska et al., 2005; Uemura et al., 2009). Here, we assessed
319 whether the observed increase in the Aβ42/40 ratio in mouse ISF induced
320 by DTDP and HNE treatment *in vivo* was associated with a similar
321 change in PS1 conformation. The brain sections of mice used for the microdialysis
322 were immunostained with PS1 antibodies to fluorescently label the N-terminus (NT)
323 and C-terminus (CT) of PS1. *Ex vivo* tissue fluorescent lifetime microscopy (FLIM)
324 was performed to determine the relative proximity between PS1-NT and -CT (PS1
325 conformation), which we expressed as FRET efficiency, %E_{FRET}, (see Methods) in
326 individual neurons of the CA1 region of the hippocampus. We found that
327 both DTDP and HNE significantly increase the mean %E_{FRET} values in
328 the neurons of CA1 area compared to the vehicle treatment (Fig. 3A).
329

This suggests that oxidative stress triggers pathogenic, “closed”, confor- 330
mational change in PS1 molecules, which in turn relates to the observed 331
increase in Ab42/40 ratio (Fig. 1C). To show the distribution of neurons 332
with PS1 in predominantly “closed” or “open” conformations, the mean 333
%E_{FRET} for each individual neuron was color-coded and mapped over the 334
CA1 area analyzed by FLIM. Fig. 3B shows a higher number of neurons 335
with pathogenic “closed” PS1 conformation (higher %E_{FRET}, color- 336
coded in yellow-red) in the hemisphere where oxidative stress was 337
induced. 338

To assess possible glia activation after the oxidative stress induction, 339
the same brains treated with HNE or DTDP by microdialysis were im- 340
munostained with astrocytic (GFAP) and microglial (Iba1) markers. 341
We did not observe any significant increase in the GFAP or Iba1 levels 342
in the HNE treated hemispheres after 6 h treatment (Supplementary 343
Fig. 1). However, a significant increase in the GFAP immunoreactivity 344
was detected in the DTDP treated hemispheres (Supplementary 345
Fig. 1), suggesting an astrocytic response to this compound. 346

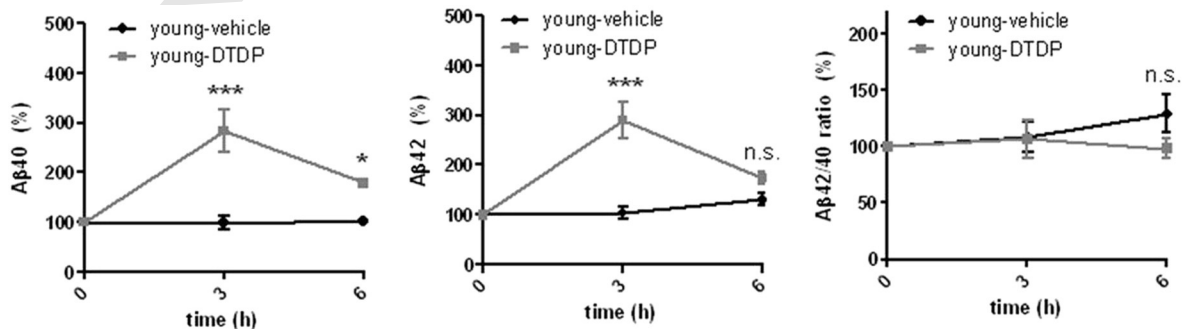


Fig. 2. Response to acute oxidative stress in young wild-type mice. ISF Aβ40, Aβ42 levels and the Aβ42/40 ratio after DTDP treatment delivered via the microdialysis probe to the brain of young (4 months old) wild-type mice (n = 3–4 animals). The baseline levels of ISF Aβ40 and Aβ42 at the time point zero were 15.28 ± 1.19 pM and 4.68 ± 0.70 pM, respectively. Data represent the mean ± SEM, presented as percentage values relative to the time point zero of each hemisphere. Two-way ANOVA, Bonferroni posttest. *p < 0.05, **p < 0.01, ***p < 0.001, compared to the same time point of the vehicle-treated hemisphere.

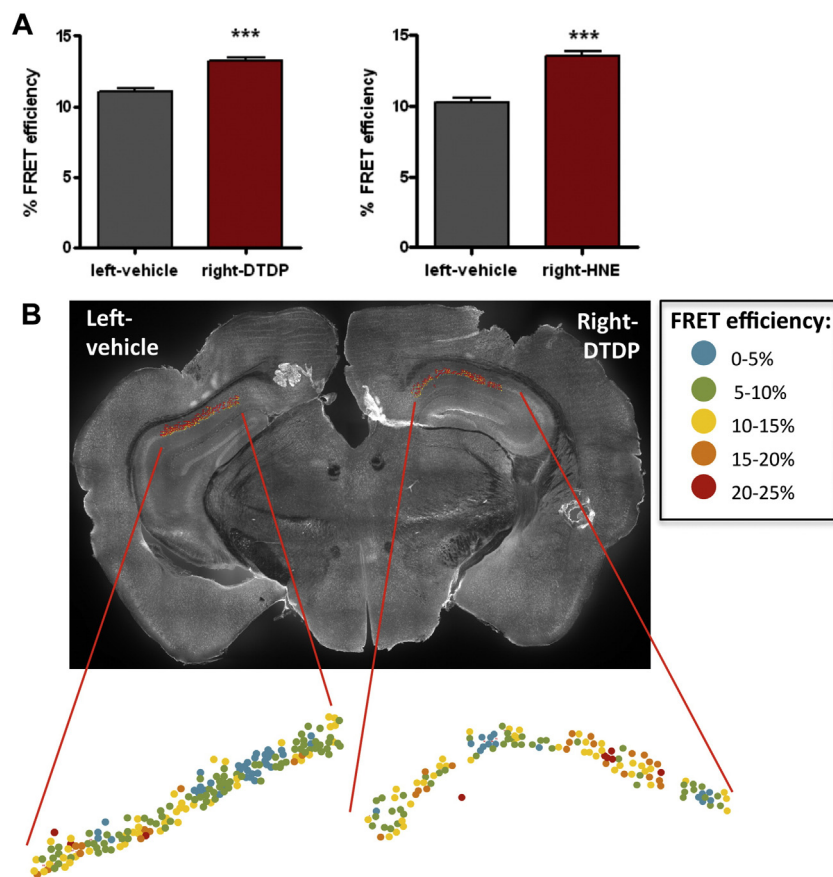


Fig. 3. Locally induced oxidative stress *in vivo* alters PS1 conformation. PS1 conformation in neurons of the CA1 area of hippocampus was assessed by FLIM analysis 6 h after the treatment with DTDP or HNE by microdialysis. (A) FRET efficiency (%) values representing proximity between PS1 NT and CT in neurons, treated with vehicle control (left hemisphere) or DTDP/HNE (right hemisphere). Data represent the mean \pm SEM of at least three different brains. *t*-Test nonparametric: Mann Whitney test. ****p* < 0.001, compared to vehicle-treated hemisphere. (B) Representative image of a brain section immunostained with PS1-NT and -CT antibodies after DTDP treatment by microdialysis. Map of the distribution of neurons within CA1 area shows color-coded % E_{FRET} values as determined by FLIM analysis.

3.3. Antioxidant NACA prevents HNE-induced changes in A β levels and in PS1 conformation

To confirm that the observed changes in the ISF A β 42 levels are produced by oxidative stress, the antioxidant N-acetylcysteine amide (NACA) (7.5 mM) was delivered to the brain via microdialysis prior to the administration of HNE (Fig. 4A). This pretreatment with NACA completely abolished the effect of HNE on A β 42 levels (Fig. 4B), whereas pretreatment with the vehicle had no effect, demonstrating that oxidative stress is the major culprit for observed increase in the A β 42 level and the A β 42/40 ratio. It should be noted that HNE itself is not a free radical but rather a product of arachidonic acid oxidation, an α,β -unsaturated hydroxyalkenal, that is significantly elevated during oxidative stress. The free thiol of NACA binds to HNE by Michael addition, preventing the reaction of HNE with proteins that affects their structure and function (Subramaniam et al., 1997; Sun, 2010). Therefore, antioxidants containing thiols, such as NACA, are the most effective in protecting against HNE damage.

Since antioxidant treatment was able to halt increase of the A β 42/40 ratio, we next examined whether NACA would also prevent HNE-induced changes in the PS1 conformation. Indeed, the mean FRET efficiency found in the NACA-HNE treated hemisphere was significantly lower compared to the vehicle-HNE treated hemisphere (Fig. 4 C-D, color-coded in blue-green), suggesting that antioxidant NACA is able to prevent HNE-induced "closed" pathogenic conformational change of PS1.

3.4. HNE treatment inhibits γ -secretase activity

To better understand the mechanism(s) by which oxidative stress affects PS1 and A β levels, we next evaluated whether DTDP and HNE may have a direct effect on γ -secretase. First, we monitored the expression level of γ -secretase components in mouse primary neurons treated with DTDP or HNE, and did not find significant changes in the PS1, NCT or Pen2 protein expression levels due to oxidative stress (data not shown). Furthermore, neither DTDP nor HNE affected the mobility of the γ -secretase complex to migrate on a native gel (Supplementary Fig. 2), suggesting that there is no drastic structural alteration of the complex.

Next, we assessed whether DTDP or HNE affect activity of the γ -secretase using membrane-enriched fractions purified from wild-type mouse brains. To bypass the effect of BACE, membrane-enriched fractions were incubated with equal amounts of human APP C100-flag peptide, an immediate substrate of the γ -secretase, and treated with DTDP, HNE or vehicle control for 4 h. A β measurements show that the HNE treatment triggers a drastic decrease in the level of both A β 40 and A β 42, similar to that achieved by treatment with the γ -secretase inhibitor (GSI) L-685,458, or by incubation at 4 °C (negative controls) (Fig. 5A). In contrast, DTDP did not significantly alter the levels of A β 40 and A β 42 in the cell-free γ -secretase activity assay.

To further evaluate the effect of oxidative stress on γ -secretase activity, a flag-tagged APP C99 fragment (C99-flag) was transiently transfected into HEK293 cells prior to treatment with either DTDP or

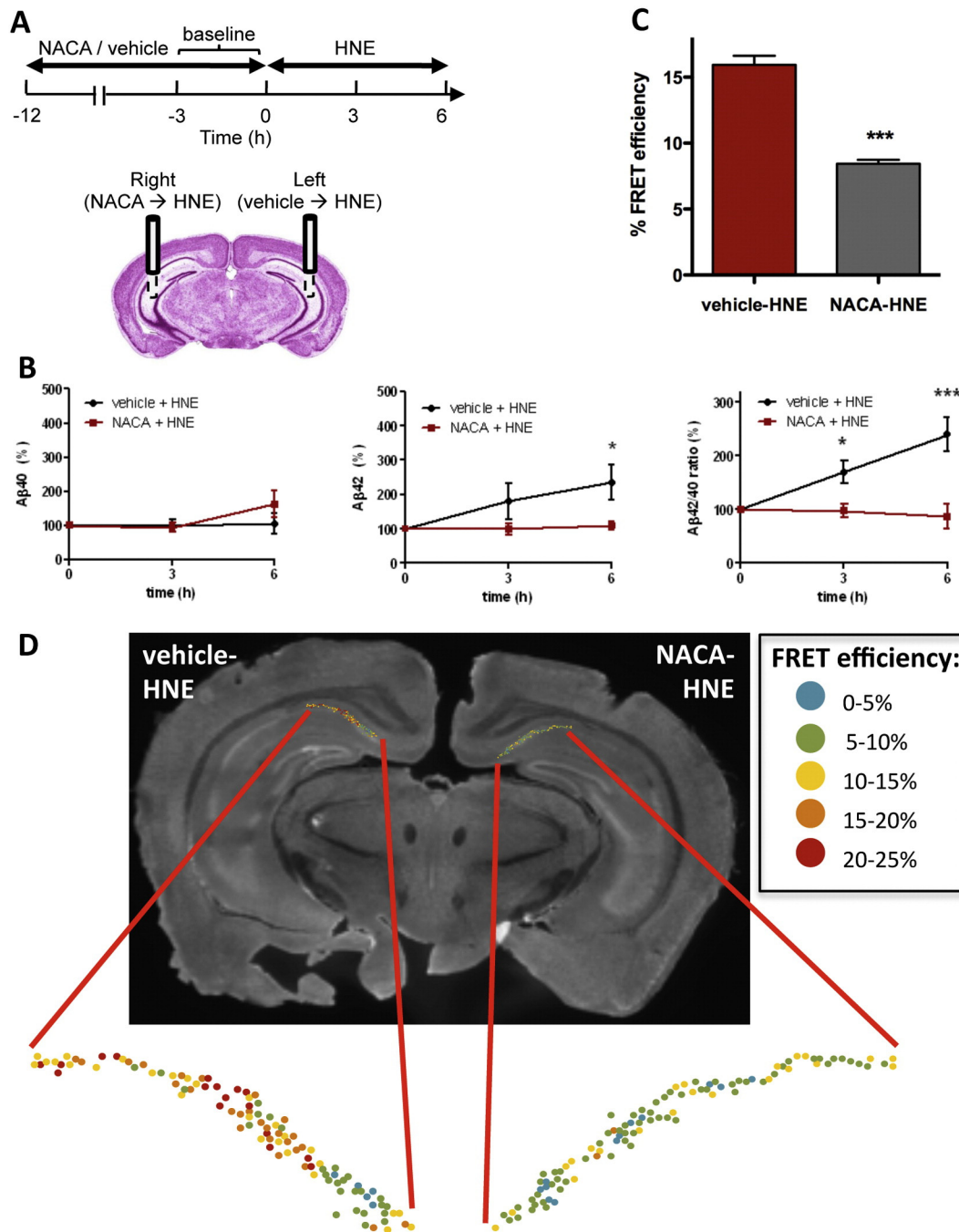


Fig. 4. Antioxidant NACA pretreatment precludes HNE effect on A β and PS1 conformation. (A) Scheme of the experiment with NACA/vehicle pretreatment prior to the HNE delivery. (B) Levels of A β 40 and A β 42 in the ISF and the A β 42/40 ratio after vehicle-HNE and NACA-HNE treatment (n = 4–5 animals). (C) FRET efficiency (%) values in neurons of the vehicle-HNE treated (left) or NACA-HNE (right) hemispheres. Data represent the mean \pm SEM. *t*-Test nonparametric: Mann Whitney test. **p* < 0.05, ****p* < 0.001, compared to vehicle-treated hemisphere; n = 3 brains. (D) Representative image of a brain section immunostained with PS1-NT and -CT antibodies after vehicle-HNE and NACA-HNE treatment by microdialysis. Map of the distribution of neurons within hippocampal CA1 area shows color-coded % E_{FRET} values as determined by FLIM analysis.

HNE. Consistent with the findings in the cell-free assay, we found that HNE causes significant accumulation of the C99-flag (Fig. 5B) as compared to the vehicle control, further supporting our finding of impaired γ -secretase activity by HNE. There was no statistically significant effect of DTDP on the C99-flag levels after 3 h of the treatment.

To determine whether HNE exerts its effect on γ -secretase via direct modification of the complex, γ -secretase was immunoprecipitated from DTDP or HNE treated neurons, and the eluates were probed for HNE adducts. No HNE adducts were found on PS1, the catalytic subunit of the complex, or Pen2. However, a significant increase in the HNE adducts

levels was detected on nicastrin (NCT) (Fig. 6). These data suggest that NCT modification by HNE could affect γ -secretase activity.

3.5. Effect of HNE and DTDP on β -secretase

Next we examined whether BACE level or activity were affected by DTDP or HNE. Treatment of primary neurons with DTDP or HNE showed no significant difference in the BACE level as compared to that in the vehicle treated cells (Fig. 7A). To evaluate BACE activity independently of γ -secretase, primary neurons were pretreated overnight with the

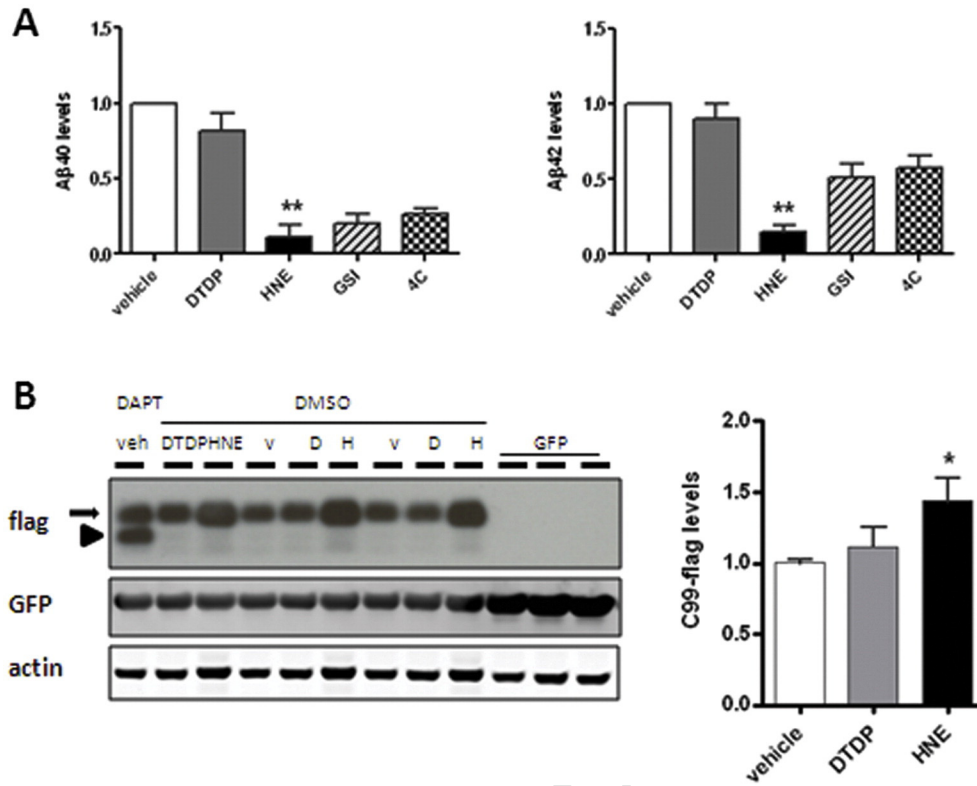


Fig. 5. Effect of DTDP and HNE on γ -secretase. (A) Cell-free γ -secretase activity assay. Membrane-enriched fractions extracted from wild-type mouse brains were incubated with the substrate C100-flag and treated with vehicle, DTDP (100 μ M) or HNE (1 mM). Treatment with the γ -secretase inhibitor L-685,458 (50 nM) or incubation at 4 $^{\circ}$ C were used as negative controls. A β 40 and A β 42 levels are shown as values relative to the vehicle treatment. Data represent the mean \pm SEM of five independent experiments. *t*-Test: **p* < 0.05, ***p* < 0.01, compared to vehicle treatment. (B) HEK293 cells co-transfected with C99-flag and GFP plasmids were treated with vehicle, DTDP or HNE. The levels of C99-flag (arrow) were quantified and normalized to GFP (transfection efficiency) and to actin (loading control). C83-flag fragment is shown by an arrowhead. Data represent the mean \pm SEM (relative to vehicle) of four independent experiments performed in triplicate. *t*-Test: **p* < 0.05, compared to vehicle treatment.

415 γ -secretase inhibitor DAPT and the level of endogenous APP C99 frag- 419
 416 ments was compared between vehicle and DTDP or HNE treated sam- 420
 417 ples. The APP C99 level was significantly elevated in the DAPT + HNE 421
 418 treated cells, compared to the DAPT + vehicle controls (Fig. 7B), 422

suggesting an increase in the BACE activity triggered by HNE. No differ- 419
 ence in C99 levels was observed after the DTDP treatment. 420

Interestingly, we found that BACE is also directly modified by HNE, 421
 as determined by significantly higher amount of the HNE adducts on 422

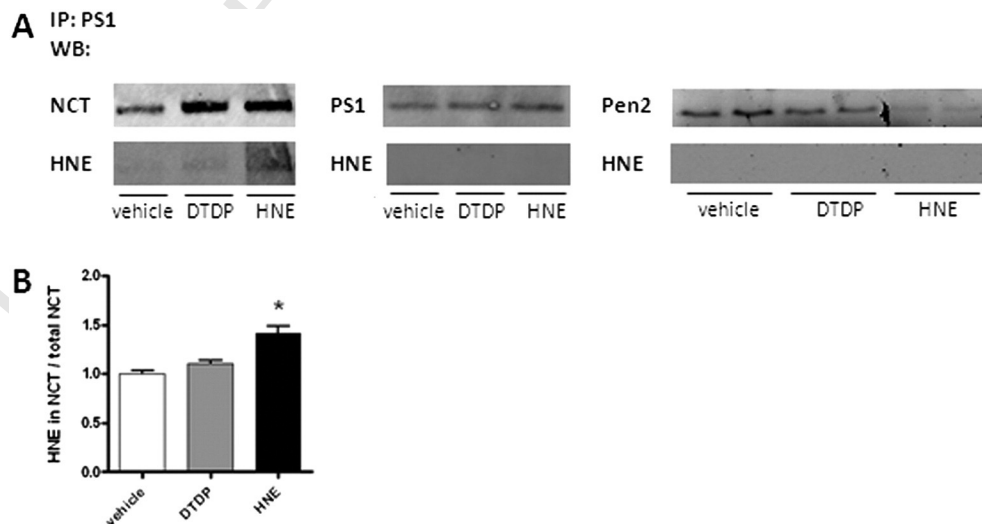


Fig. 6. HNE covalently modifies nicastrin. γ -secretase complexes were immunoprecipitated from primary neurons treated with vehicle, DTDP or HNE using PS1-NT and PS1-loop antibodies. (A) Immunoblots were simultaneously probed with the corresponding antibodies to NCT, PS1 and Pen2, and with an antibody specific to HNE adducts. The Li-Cor Odyssey infrared imaging system was used to detect HNE adducts on exactly the same bands of NCT, PS1 and Pen2, respectively. (B) The HNE levels were normalized to the immunoprecipitated NCT levels. There was no detectable HNE signal on PS1 and Pen2 bands. Data represent the mean \pm SEM (relative to vehicle) of three independent experiments. *t*-Test: **p* < 0.05, compared to vehicle treatment.

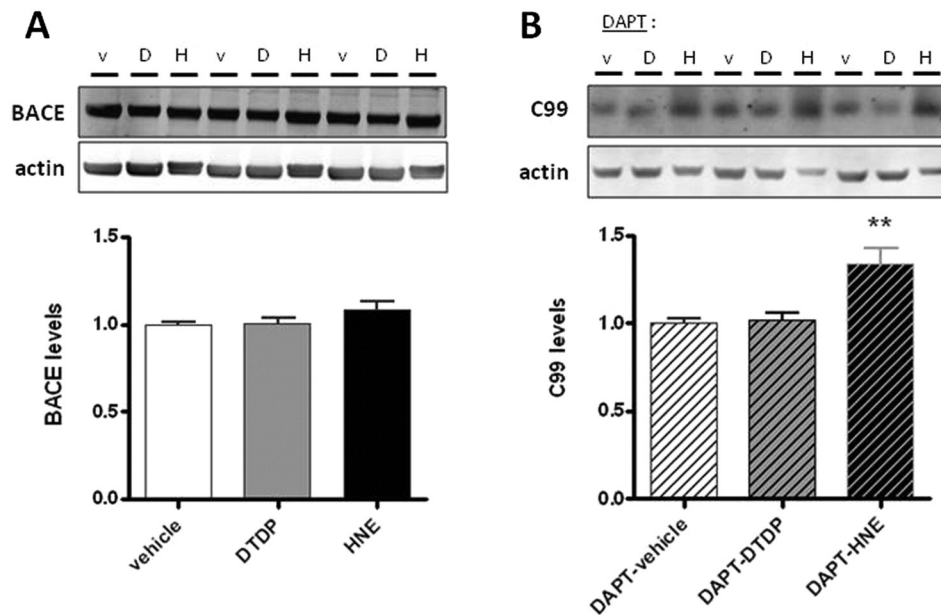


Fig. 7. Effect of DTDP and HNE on BACE. (A) Western blot analysis of BACE protein levels in primary neurons after DTDP or HNE treatment. (b) Primary neurons were pre-treated overnight with DAPT before incubation with DTDP or HNE, and the amount of APP C99 fragments was quantified by a C99 specific antibody. Data represent the mean \pm SEM (relative to vehicle) of three independent experiments performed at least in triplicates. *t*-Test: ***p* < 0.01, compared to vehicle treatment.

423 BACE immunoprecipitated from primary neurons treated with HNE,
 424 compared to that in DTDP or vehicle treated cells (Fig. 8). This suggests
 425 that covalent modification of BACE by HNE adducts may lead to the ab-
 426 normal increase in its enzymatic activity.

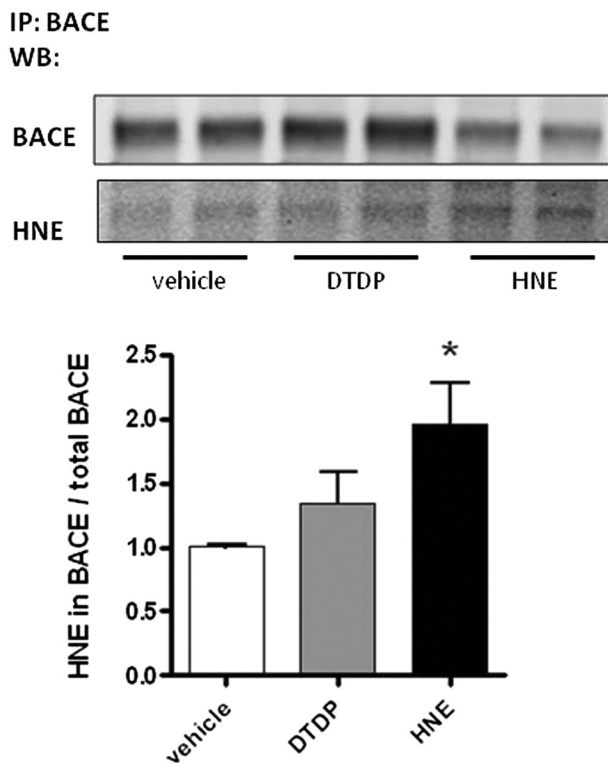


Fig. 8. HNE covalently modifies BACE. BACE was immunoprecipitated from primary neurons treated with DTDP or HNE. Immunoblots were simultaneously probed with antibodies specific to BACE and to HNE adducts, using the Li-Cor Odyssey infrared imaging system. The HNE levels were normalized to the immunoprecipitated BACE levels. Data represent the mean \pm SEM (relative to vehicle) of four independent experiments. *t*-Test: **p* < 0.05, compared to vehicle treatment.

4. Discussion

427

To determine the relationship between oxidative stress and A β pathology, and to establish whether oxidative stress, and specifically lipid peroxidation, may be an initiator of A β pathology, we employed *in vivo* microdialysis to locally induce acute oxidative stress in the brains of awake mice using a naturally occurring product of lipid peroxidation, HNE (Sayre et al., 1997; Cutler et al., 2004; Williams et al., 2006), and a strong thiol-reactive agent, DTDP. Our results show that both compounds alter the ISF levels of A β within 3–6 h of treatment. Importantly, both HNE and DTDP significantly increased the level of highly fibrillogenic A β species, A β 42, and resulted in elevated A β 42/40 ratio *in vivo*. The A β 42/40 ratio, rather than total absolute A β levels, has been reported to play a crucial role in A β deposition and neurodegeneration (Borchelt et al., 1996; Lewczuk et al., 2004; Wiltfang et al., 2007; Wolfe, 2007; Kuperstein et al., 2010). It has been previously shown that the A β 42/40 ratio strongly correlates with the conformation of PS1/ γ -secretase in cells *in vitro* (Lleo et al., 2004; Berezovska et al., 2005; Isoo et al., 2007; Serneels et al., 2009), proposing that pathogenic structural changes may affect the γ -secretase cleavage site. Indeed, in a recent study, we found that changes in conformation of endogenous PS1 do occur in normal aging in mouse brain and in sporadic AD patients (Wahlster et al., 2013). Moreover, we observed more pronounced PS1 conformational changes in close proximity to amyloid plaques, suggesting a link between the microenvironment surrounding A β plaques, PS1 conformation and A β deposition in AD brain (Wahlster et al., 2013). Concurring with these findings, here we detect a similar pathogenic “closed” PS1 configuration in the hippocampus of mice treated with the oxidative agents DTDP and HNE. This observation strongly supports the hypothesis that changes in conformation of PS1/ γ -secretase, and consequent elevation in the A β 42/40 ratio could be early events occurring due to local increase in the oxidative stress and its products in the brain. Indeed, pretreatment with antioxidant NACA prior to the HNE insult completely abolished HNE-triggered increase in the A β 42 and A β 42/40 ratio, as well as prevented change in the PS1 conformation, confirming the specificity of the observed effect. Along the same lines, we found that young mice were able to recover from the insult faster than the old animals, most likely due to presence of stronger antioxidant defense mechanisms in the former.

464

465 HNE, a by-product of lipid peroxidation, has been shown to accumu- 502
 466 late in membranes at concentrations of 10 μ M to 5 mM in response to 503
 467 oxidative insults (Esterbauer et al., 1991; Uchida, 2003). HNE is relative- 504
 468 ly stable and can transfer between subcellular compartments; thereby 505
 469 having the potential to interact with many different proteins within 506
 470 the cell. It can react with the histidine, lysine and cysteine protein resi-
 471 dues to generate stable adducts, resulting in alterations in the protein
 472 structure and function (Esterbauer et al., 1991; Subramaniam et al.,
 473 1997; Tamagno et al., 2002; Uchida, 2003). Here, we show that HNE direct-
 474 ly modifies the γ -secretase component NCT in primary neurons. This
 475 finding is in agreement with a previous report showing that NCT
 476 is also modified by HNE in AD brain specimens (Gwon et al., 2012).
 477 Modifications of the γ -secretase complex components, such as intro-
 478 ducing mutations into PS1 (Berezovska et al., 2005), Pen2 NT extension
 479 (Isoo et al., 2007; Uemura et al., 2009), or expressing different Aph1 iso-
 480 forms (Serneels et al., 2009), have been shown to affect the conforma-
 481 tion of PS1/ γ -secretase and hence, the A β species generated. Now we
 482 propose that covalent modifications of NCT by the product of lipid per-
 483 oxidation HNE, can also trigger similar pathogenic conformational
 484 changes.

485 We have also recently reported that peroxynitrite, an oxidant that accu- 523
 486 mulates during aging, induces PS1 conformational changes in cells 524
 487 *in vitro*, resulting in changes in the A β 42/40 ratio (Guix et al., 2012). 525
 488 Together, these data suggest that the effect of oxidative stress on PS1/
 489 γ -secretase might be a common pathogenic outcome, rather than
 490 being limited to a specific oxidation product (e.g. HNE) or specific reac-
 491 tive oxygen species.

492 HNE adducts are known to alter the activity of a variety of enzymes 529
 493 (reviewed in (Tamagno et al., 2002; Uchida, 2003)). Indeed, we found 530
 494 that HNE modified the activity of both β - and γ -secretase. Unlike the 531
 495 study of Gwon et al. (Gwon et al., 2012), however, we found that 532
 496 HNE significantly impaired γ -secretase activity both in a cellular envi-
 497 ronment and in a cell free assay by causing structural change of the
 498 γ -secretase complex similar to that of FAD PS1 mutations. It is believed
 499 that FAD mutations in PS1 as well as pathogenic changes in PS1/
 500 γ -secretase in sporadic AD, may lead to a partial loss of function
 501 (Wang et al., 2006; De Strooper, 2007; Shen and Kelleher, 2007;

Kelleher and Shen, 2010; Xia et al., 2015). Indeed, many FAD PS1 muta- 502
 tions result in reduced overall A β production, however the ratio of the 503
 longer A β 42 and A β 43 species to A β 40/total is steadily increased 504
 (Wang et al., 2006; De Strooper, 2007; Shen and Kelleher, 2007; 505
 Kelleher and Shen, 2010; Xia et al., 2015). 506

507 On the other hand, the activity of β -secretase was intensified by HNE 507
 adducts covalently linked to the BACE protein in primary neurons. To 508
 the best of our knowledge, this is the first time that the HNE adducts 509
 are detected on the β -secretase enzyme, providing a molecular mecha- 510
 nism by which oxidative stress may affect BACE activity. This finding is 511
 consistent with previous studies showing that H₂O₂/FeSO₄ induced ox- 512
 idative stress and generation of HNE increases β -secretase activity in 513
 NT₂ cells (Gwon et al., 2012). We did not observe any significant change 514
 in the BACE levels within three hours of treatment of primary neurons 515
 with HNE; although studies by Tamagno et al. (Tamagno et al., 2002; 516
 Tamagno et al., 2005) reported an increase in the BACE levels in NT₂ 517
 cells *in vitro* after 1 hr of HNE treatment. It is worth mentioning that 518
 in our experimental conditions HNE did not modify APP or C99 519
 fragment (Supplementary Fig. 3) or any of the other components in 520
 the γ -secretase complex apart from NCT (Fig. 5), hence ruling out an ex- 521
 tensive non-specific effect of HNE. 522

523 Although DTDP significantly altered A β levels in the mouse brain 523
in vivo, it did not have any significant effect on either γ -secretase or 524
 BACE activity in cells or cell-free assay *in vitro*. Since increased GFAP im- 525
 munoreactivity was detected in DTDP treated hemispheres within 6 h of 526
 perfusion, it is plausible that astrocyte activation may mediate the DTDP 527
 effect on A β in the brain. Indeed, a number of studies reported a role of 528
 astrocytes in elevating A β levels (Mark et al., 1997a; Tamagno et al., 529
 2005; Wang et al., 2006; Shen and Kelleher, 2007; Kelleher and Shen, 530
 2010). It is also feasible that DTDP alters A β clearance, which would ex- 531
 plain the increase in A β levels observed *in vivo* but not *in vitro*. Different 532
 clearance rates for A β 40 versus A β 42 could also explain an altered 533
 A β 42/40 ratio. 534

535 Taken together, our results suggest a model (Fig. 9) in which HNE 535
 resulting from increased lipid peroxidation (due to aging, decreased 536
 antioxidant defenses, inflammation processes, etc.) covalently attaches 537
 and modifies both γ -secretase and BACE. These modifications 538

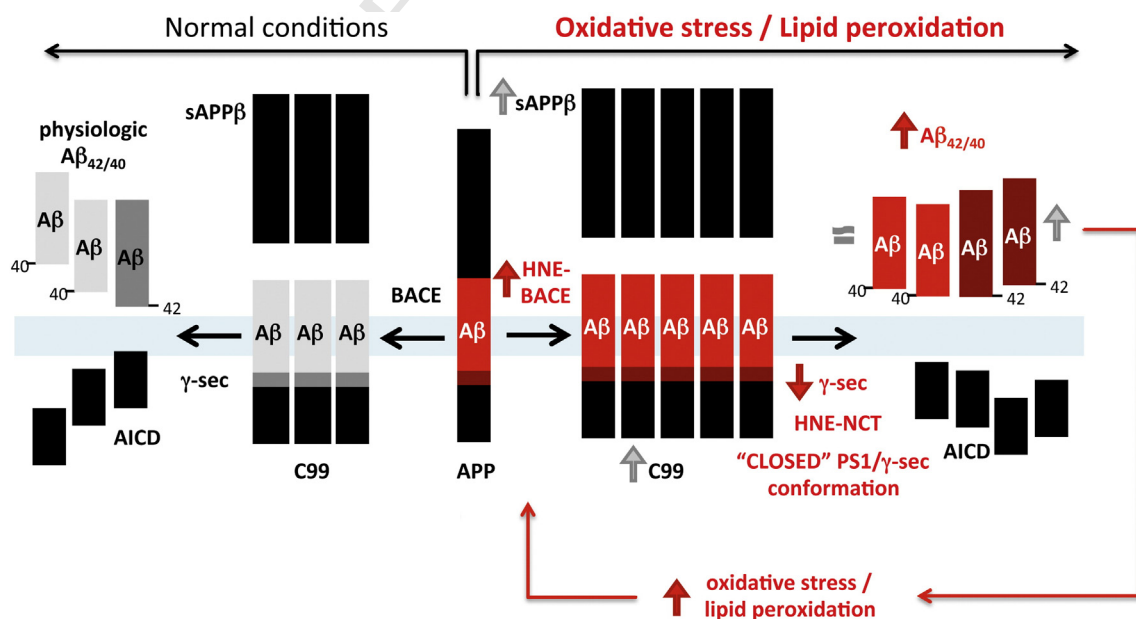


Fig. 9. Schematic representation of the effect of HNE on A β production. We propose that HNE resulting from lipid peroxidation covalently modifies both BACE and nicastrin/ γ -secretase. As a result, β -secretase activity is enhanced, whereas γ -secretase activity is decreased. Therefore, the total A β levels in the brain may not significantly change due to this "bottle-neck" effect. At the same time, the HNE modification of NCT triggers a pathogenic change in PS1/ γ -secretase conformation, similar to that of FAD PS1 mutations, resulting in increased A β 42 generation and higher A β 42/40 ratio.

differentially affect their activity, causing an increase in BACE activity but on the other hand, inflict γ -secretase conformational changes leading to decreased activity. Therefore, the total A β levels in the brain may not be significantly altered because of a “bottle-neck” effect, i.e. increased β -secretase but decreased γ -secretase activities. In addition, oxidative stress induced impairment of the A β clearance/degradation in the brain may somewhat hide PS1/ γ -secretase loss-of-activity phenomena. However, the γ -secretase cleavage site on APP is altered as a consequence of NCT subunit modification by the HNE adducts, or as previously reported by nitrotyrosination of PS1 (Guix et al., 2012), causing compression of the complex (detected as “closed” PS1 conformation) and partial loss of its activity. In accord with the step-wise cleavage model (Chavez-Gutierrez et al., 2012), less active γ -secretase stops at producing longer A β species, resulting in higher A $\beta_{42/40}$ ratio. This is also in agreement with the hypothesis of qualitative rather than quantitative shifts in the A β profiles representing pathogenic effect of all FAD mutations (Chavez-Gutierrez et al., 2012). Altered ratio of longer A β species (A $\beta_{42/43}$) to shorter (A β_{40}) rather than total A β is associated with increased neurotoxicity and amyloid deposition. In turn, A β itself can induce oxidative stress/membrane lipid peroxidation and HNE production in neurons (Mark et al., 1997a, 1997b). Thus, an initial local oxidative insult may initiate a feed-forward loop triggering and/or worsening amyloid pathology, creating a vicious cycle.

In conclusion, our study demonstrates a direct causative relationship between oxidative stress and lipid peroxidation, changes in conformation of PS1/ γ -secretase and amyloid pathology, and proposes a molecular mechanism by which the lipid peroxidation product, HNE, affects the generation of toxic A β_{42} species.

Supplementary data to this article can be found online at <http://dx.doi.org/10.1016/j.nbd.2015.06.013>.

Author contributions

M.A. and O.B. designed the experiments, M.A., S.T., K.L.P., and S.S. performed experiments and analyzed the data; M.A. and O.B. wrote the manuscript. O.B., M.A., S.T., and B.T.H. discussed the results, provided constructive criticism of the findings, and commented on the manuscript.

Conflict of interest

The authors declare that they have no conflict of interest.

Acknowledgments

We would like to thank Dr. Alberto Serrano-Pozo, MD, PhD, for helpful discussions. This work was supported by National Institutes of Health grants [AG044486 and AG15379 to O.B.]; funding from BrightFocus foundation [O.B.], and the MGH ECOR Postdoctoral Fellowship Award [Fund for Medical Discovery to M.A.].

References

- Atamna, H., Boyle, K., 2006. Amyloid-beta peptide binds with heme to form a peroxidase: relationship to the cytopathologies of Alzheimer's disease. *Proc. Natl. Acad. Sci. U. S. A.* 103 (9), 3381–3386.
- Berezovska, O., Frosch, M., et al., 1999. The Alzheimer-related gene presenilin 1 facilitates notch 1 in primary mammalian neurons. *Brain Res. Mol. Brain Res.* 69 (2), 273–280.
- Berezovska, O., Lleo, A., et al., 2005. Familial Alzheimer's disease presenilin 1 mutations cause alterations in the conformation of presenilin and interactions with amyloid precursor protein. *J. Neurosci.* 25 (11), 3009–3017.
- Bergmans, B.A., De Strooper, B., 2010. gamma-secretases: from cell biology to therapeutic strategies. *Lancet Neurol.* 9 (2), 215–226.
- Borchelt, D.R., Thinakaran, G., et al., 1996. Familial Alzheimer's disease-linked presenilin 1 variants elevate Abeta1-42/1-40 ratio in vitro and in vivo. *Neuron* 17 (5), 1005–1013.
- Butterfield, D.A., 2002. Amyloid beta-peptide (1-42)-induced oxidative stress and neurotoxicity: implications for neurodegeneration in Alzheimer's disease brain. A review. *Free Radic. Res.* 36 (12), 1307–1313.

- Butterfield, D.A., Hensley, K., et al., 1997. Oxidatively induced structural alteration of glutamine synthetase assessed by analysis of spin label incorporation kinetics: relevance to Alzheimer's disease. *J. Neurochem.* 68 (6), 2451–2457.
- Butterfield, D.A., Griffin, S., et al., 2002. Amyloid beta-peptide and amyloid pathology are central to the oxidative stress and inflammatory cascades under which Alzheimer's disease brain exists. *J. Alzheimers Dis.* 4 (3), 193–201.
- Butterfield, D.A., Reed, T., et al., 2006. Elevated protein-bound levels of the lipid peroxidation product, 4-hydroxy-2-nonenal, in brain from persons with mild cognitive impairment. *Neurosci. Lett.* 397 (3), 170–173.
- Cai, Z., Zhao, B., et al., 2011. Oxidative stress and beta-amyloid protein in Alzheimer's disease. *Neuromol. Med.* 13 (4), 223–250.
- Chavez-Gutierrez, L., Bammens, L., et al., 2012. The mechanism of gamma-Secretase dysfunction in familial Alzheimer disease. *EMBO J.* 31 (10), 2261–2274.
- Cirrito, J.R., May, P.C., et al., 2003. In vivo assessment of brain interstitial fluid with microdialysis reveals plaque-associated changes in amyloid-beta metabolism and half-life. *J. Neurosci.* 23 (26), 8844–8853.
- Cutler, R.G., Kelly, J., et al., 2004. Involvement of oxidative stress-induced abnormalities in ceramide and cholesterol metabolism in brain aging and Alzheimer's disease. *Proc. Natl. Acad. Sci. U. S. A.* 101 (7), 2070–2075.
- De Strooper, B., 2007. Loss-of-function presenilin mutations in Alzheimer disease. *Talking Point on the role of presenilin mutations in Alzheimer disease.* *EMBO Rep.* 8 (2), 619–620.
- Esterbauer, H., Schaur, R.J., et al., 1991. Chemistry and biochemistry of 4-hydroxynonenal, malonaldehyde and related aldehydes. *Free Radic. Biol. Med.* 11 (1), 81–128.
- Finkel, T., Holbrook, N.J., 2000. Oxidants, oxidative stress and the biology of ageing. *Nature* 408 (6809), 239–247.
- Garcia-Alloza, M., Dodwell, S.A., et al., 2006. Plaque-derived oxidative stress mediates distorted neurite trajectories in the Alzheimer mouse model. *J. Neuropathol. Exp. Neurol.* 65 (11), 1082–1089.
- Guix, F.X., Wahle, T., et al., 2012. Modification of gamma-secretase by nitrosative stress links neuronal ageing to sporadic Alzheimer's disease. *EMBO Mol. Med.* 4 (7), 660–673.
- Gwon, A.R., Park, J.S., et al., 2012. Oxidative lipid modification of nicastrin enhances amyloidogenic gamma-secretase activity in Alzheimer's disease. *Aging Cell* 11 (4), 559–568.
- Hardy, J., Selkoe, D.J., 2002. The amyloid hypothesis of Alzheimer's disease: progress and problems on the road to therapeutics. *Science* 297 (5580), 353–356.
- Harris, M.E., Hensley, K., et al., 1995. Direct evidence of oxidative injury produced by the Alzheimer's beta-amyloid peptide (1-40) in cultured hippocampal neurons. *Exp. Neurol.* 131 (2), 193–202.
- Isoo, N., Sato, C., et al., 2007. Abeta42 overproduction associated with structural changes in the catalytic pore of gamma-secretase: common effects of Pen-2 N-terminal elongation and fenofibrate. *J. Biol. Chem.* 282 (17), 12388–12396.
- Kelleher III, R.J., Shen, J., 2010. Genetics. Gamma-secretase and human disease. *Science* 330 (6007), 1055–1056.
- Krstic, D., Knuesel, I., 2013. Deciphering the mechanism underlying late-onset Alzheimer disease. *Nat. Rev. Neurol.* 9 (1), 25–34.
- Kuperstein, I., Broersen, K., et al., 2010. Neurotoxicity of Alzheimer's disease Abeta peptides is induced by small changes in the Abeta42 to Abeta40 ratio. *EMBO J.* 29 (19), 3408–3420.
- Lewczuk, P., Esselmann, H., et al., 2004. Neurochemical diagnosis of Alzheimer's dementia by CSF Abeta42, Abeta42/Abeta40 ratio and total tau. *Neurobiol. Aging* 25 (3), 273–281.
- Lleo, A., Berezovska, O., et al., 2004. Nonsteroidal anti-inflammatory drugs lower Abeta42 and change presenilin 1 conformation. *Nat. Med.* 10 (10), 1065–1066.
- Lovell, M.A., Markesbery, W.R., 2001. Ratio of 8-hydroxyguanine in intact DNA to free 8-hydroxyguanine is increased in Alzheimer disease ventricular cerebrospinal fluid. *Arch. Neurol.* 58 (3), 392–396.
- Mangialasche, F., Polidori, M.C., et al., 2009. Biomarkers of oxidative and nitrosative damage in Alzheimer's disease and mild cognitive impairment. *Ageing Res. Rev.* 8 (4), 658–659.
- Mark, R.J., Lovell, M.A., et al., 1997a. A role for 4-hydroxynonenal, an aldehydic product of lipid peroxidation, in disruption of ion homeostasis and neuronal death induced by amyloid beta-peptide. *J. Neurochem.* 68 (1), 255–264.
- Mark, R.J., Pang, Z., et al., 1997b. Amyloid beta-peptide impairs glucose transport in hippocampal and cortical neurons: involvement of membrane lipid peroxidation. *J. Neurosci.* 17 (3), 1046–1054.
- McLellan, M.E., Kajdasz, S.T., et al., 2003. In vivo imaging of reactive oxygen species specifically associated with thioflavine S-positive amyloid plaques by multiphoton microscopy. *J. Neurosci.* 23 (6), 2212–2217.
- Nemoto, S., Takeda, K., et al., 2000. Role for mitochondrial oxidants as regulators of cellular metabolism. *Mol. Cell Biol.* 20 (19), 7311–7318.
- Nishikawa, T., Edelstein, D., et al., 2000. Normalizing mitochondrial superoxide production blocks three pathways of hyperglycaemic damage. *Nature* 404 (6779), 787–790.
- Pratico, D., Uryu, K., et al., 2001. Increased lipid peroxidation precedes amyloid plaque formation in an animal model of Alzheimer amyloidosis. *J. Neurosci.* 21 (12), 4183–4187.
- Reed, T.T., Pierce Jr., W.M., et al., 2009a. Proteomic identification of nitrated brain proteins in early Alzheimer's disease inferior parietal lobule. *J. Cell. Mol. Med.* 13 (8B), 678–679.
- Reed, T.T., Pierce, W.M., et al., 2009b. Proteomic identification of HNE-bound proteins in early Alzheimer disease: Insights into the role of lipid peroxidation in the progression of AD. *Brain Res.* 1274, 66–76.
- Sajdel-Sulkowska, E.M., Marotta, C.A., 1984. Alzheimer's disease brain: alterations in RNA levels and in a ribonuclease-inhibitor complex. *Science* 225 (4665), 947–949.

- 685 Sayre, L.M., Zelasko, D.A., et al., 1997. 4-Hydroxynonenal-derived advanced lipid peroxi- 714
686 dation end products are increased in Alzheimer's disease. *J. Neurochem.* 68 (5), 715
687 2092–2097. 716
- 688 Serneels, L., Van Biervliet, J., et al., 2009. gamma-Secretase heterogeneity in the Aph1 sub- 717
689 unit: relevance for Alzheimer's disease. *Science* 324 (5927), 639–642. 718
- 690 Shen, J., Kelleher 3rd, R.J., 2007. The presenilin hypothesis of Alzheimer's disease: 719
691 evidence for a loss-of-function pathogenic mechanism. *Proc. Natl. Acad. Sci. U. S. A.* 720
692 104 (2), 403–409. 721
- 693 Shichiri, M., Yoshida, Y., et al., 2011. alpha-Tocopherol suppresses lipid peroxidation and 722
694 behavioral and cognitive impairments in the Ts65Dn mouse model of Down syn- 723
695 drome. *Free Radic. Biol. Med.* 50 (12), 1801–1811. 724
- 696 Subramaniam, R., Roediger, F., et al., 1997. The lipid peroxidation product, 4-hydroxy-2- 725
697 trans-nonenal, alters the conformation of cortical synaptosomal membrane proteins. 726
698 *J. Neurochem.* 69 (3), 1161–1169. 727
- 699 Subramanian, R., Tam, J., et al., 2011. Novel cytochrome p450 bioactivation of a terminal 728
700 phenyl acetylene group: formation of a one-carbon loss benzaldehyde and other ox- 729
701 idative products in the presence of N-acetyl cysteine or glutathione. *Chem. Res.* 730
702 *Toxicol.* 24 (5), 677–686. 731
- 703 Sultana, R., Butterfield, D.A., 2010. Role of oxidative stress in the progression of 732
704 Alzheimer's disease. *J. Alzheimers Dis.* 19 (1), 341–353. 733
- 705 Sun, S.Y., 2010. N-acetylcysteine, reactive oxygen species and beyond. *Cancer Biol. Ther.* 9 734
706 (2), 109–110. 735
- 707 Takeda, S., Sato, N., et al., 2011. Novel microdialysis method to assess neuropeptides and 736
708 large molecules in free-moving mouse. *Neuroscience* 186, 110–119. **Q4**
- 709 Tamagno, E., Bardini, P., et al., 2002. Oxidative stress increases expression and activity of 737
710 BACE in NT2 neurons. *Neurobiol. Dis.* 10 (3), 279–288. 738
- 711 Tamagno, E., Parola, M., et al., 2005. Beta-site APP cleaving enzyme up-regulation induced 739
712 by 4-hydroxynonenal is mediated by stress-activated protein kinases pathways. 740
713 *J. Neurochem.* 92 (3), 628–636. 741
- Uchida, K., 2003. 4-Hydroxy-2-nonenal: a product and mediator of oxidative stress. *Prog. 714
Lipid Res.* 42 (4), 318–343. 715
- Uemura, K., Lill, C.M., et al., 2009. Allosteric modulation of PS1/gamma-secretase confor- 716
mation correlates with amyloid beta(42/40) ratio. *PLoS One* 4 (11), e7893. 717
- Uemura, K., Farner, K.C., et al., 2010. Substrate docking to gamma-secretase allows access 718
of gamma-secretase modulators to an allosteric site. *Nat. Commun.* 1, 130. 719
- Wahlster, L., Arimon, M., et al., 2013. Presenilin-1 adopts pathogenic conformation in nor- 720
mal aging and in sporadic Alzheimer's disease. *Acta Neuropathol.* 125 (2), 187–199. 721
- Wang, R., Tang, P., et al., 2006. Regulation of tyrosinase trafficking and processing by 722
presenilins: partial loss of function by familial Alzheimer's disease mutation. *Proc.* 723
Natl. Acad. Sci. U. S. A. 103 (2), 353–358. 724
- Williams, T.L., Lynn, B.C., et al., 2006. Increased levels of 4-hydroxynonenal and acrolein, 725
neurotoxic markers of lipid peroxidation, in the brain in Mild Cognitive Impairment 726
and early Alzheimer's disease. *Neurobiol. Aging* 27 (8), 1094–1099. 727
- Wiltfang, J., Esselmann, H., et al., 2007. Amyloid beta peptide ratio 42/40 but not A beta 42 728
correlates with phospho-Tau in patients with low- and high-CSF A beta 40 load. 729
J. Neurochem. 101 (4), 1053–1059. 730
- Wolfe, M.S., 2007. When loss is gain: reduced presenilin proteolytic function leads to in- 731
creased Abeta42/Abeta40. *Talking Point on the role of presenilin mutations in* 732
Alzheimer disease. *EMBO Rep.* 8 (2), 136–140. 733
- Xia, D., Watanabe, H., et al., 2015. Presenilin-1 knockin mice reveal loss-of-function mech- 734
anism for familial Alzheimer's disease. *Neuron* 85 (5), 967–981. 735
- Xie, H., Hou, S., et al., 2013. Rapid cell death is preceded by amyloid plaque-mediated ox- 736
idative stress. *Proc. Natl. Acad. Sci. U. S. A.* 737